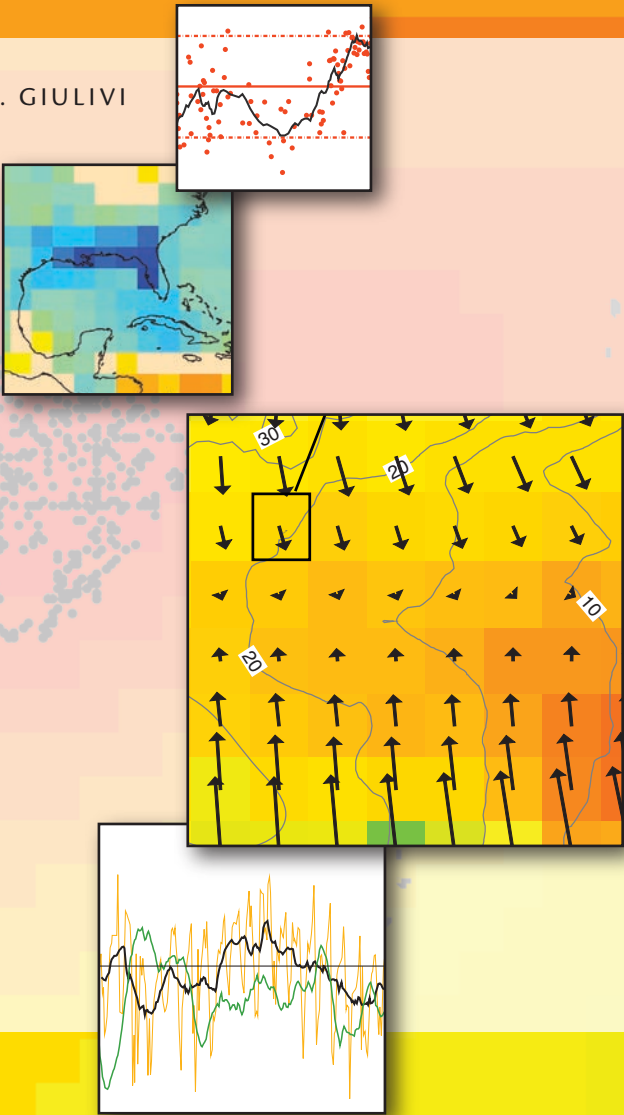


SEA SURFACE SALINITY TRENDS OVER FIFTY YEARS WITHIN THE SUBTROPICAL NORTH ATLANTIC

BY ARNOLD L. GORDON AND CLAUDIA F. GIULIVI



Seawater is a dilute salt solution. The salt or salinity¹ is reduced or elevated as freshwater is added or removed, respectively, through precipitation, evaporation, and sea-ice melting and freezing, as well as river runoff from land. If the freshwater inventory within the ocean water column remains in quasi-steady state, imbalances of sea-air flux of freshwater at specific sites are compensated with freshwater convergence or divergence by ocean currents and mixing, including eddies and wind-induced Ekman transport. Climate fluctuations alter the hydrological cycle. On land, these modifications are manifested as droughts in one region and floods in another. At sea, they alter the ocean's freshwater inventory and salinity. Considering that the ocean is about 71% of Earth's surface and that the hydrological cycle, including its relationship to latent heat transport, is so central to the climate system, the marine component of the hydrological cycle is surprisingly poorly observed. Sea-surface salinity (SSS) serves as a proxy

for the marine hydrological cycle. Salinity not only responds to the hydrological system but also is an equation-of-state parameter as it, along with temperature and pressure, determine seawater density and associated circulation and mixing dynamics. Despite these complexities, salinity is remarkably uniform on a global scale, with 99% of seawater falling within the narrow range of 33.1 to 37.2—an approximately 3.31% to 3.72% salt solution (Worthington, 1981)—attesting to the effectiveness of ocean-circulation-induced freshwater fluxes in the presence of the highly spatially variable sea-air freshwater exchange.

Rain gauges and radar systems commonly seen on TV weather reports record precipitation on the land, but over the sea, crude estimates of precipitation are drawn from averaging sparse, ship-based data and inferences from cloud cover, and more recently from satellite microwave sensors (e.g., the Tropical Rainfall Measuring Mission [TRMM, <http://trmm.gsfc.nasa.gov/>] and Earth

Observing System satellites [<http://eospso.gsfc.nasa.gov/>; <http://www.noaa.gov/eos.html>]).

The SSS spatial pattern reflects the climate belts associated with general atmospheric circulation. Comparison of SSS to net sea-air freshwater fluxes reveals remarkably similar patterns (Schmitt et al., 1989; Baumgartner and Reichel, 1975). The great subtropical deserts at the poleward edges of the atmosphere's Hadley cells are apparent over the ocean as a SSS maximum in the 15° to 30° latitude band. Tropical rain lowers the SSS along the Intertropical Convergence Zone. From the mid-latitudes to the polar regions, excess precipitation lowers SSS. The marine hydrological cycle varies in longitude, too. Net evaporation leads to a relatively salty Atlantic; net input of freshwater generates low salinity, characteristic of the Pacific Ocean (Gordon, 2001; Figure 1). Seasonal changes of SSS correspond to seasonality of precipitation, clearly evident in the monsoon climate over the ocean surrounding southern

¹ Salinity is a dimensionless oceanographic parameter that approximates the total salt content of seawater (Schmitt, 1995). The Report of the US CLIVAR Salinity Science Working Group (US CLIVAR, 2007) states: "Traditionally salinity was expressed in parts per thousand, mass per mass. In recent decades, salinity has been defined using the Practical Salinity Scale of 1978 (PSS-78) based on conductivity measurements for seawater from the North Atlantic. This nondimensional salinity scale is commonly denoted by (practical salinity unit)." Details are provided in the "Special issue on the practical salinity scale 1978" (*IEEE Journal of Oceanic Engineering* 5(1), 1980).

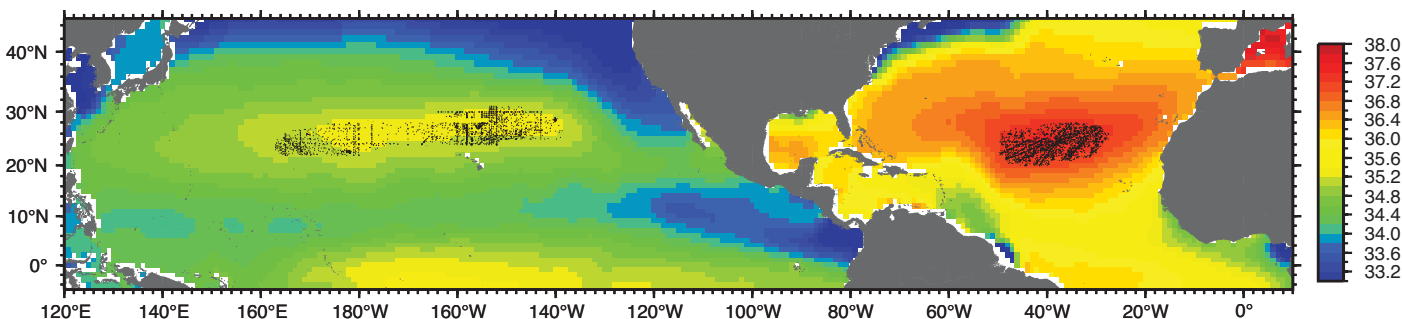


Figure 1. Annual mean sea surface salinity (SSS, defined as average salinity of the upper 20 m) from the 1° x 1° World Ocean Atlas 2005 (Boyer et al., 2006). Solid circles indicate the location of archived hydrographic stations within the North Atlantic and North Pacific subtropical gyres used to construct the SSS time series shown in Figure 2.

and southeastern Asia. Interannual and longer-term temporal fluctuations are linked to various climate indices, such as those associated with the tropical Pacific El Niño Southern Oscillation (ENSO) phenomenon.

Despite the central role that salinity plays in ocean circulation and as an indicator of the marine hydrological cycle,

Ocean Salinity mission) and the 2010 launch of Aquarius SAC-D (Lagerloef et al., 1995, this issue). Satellite data, along with improved in situ salinity sensors placed on drifting and profiling platforms such as Argo floats (see Riser et al., this issue) and gliders, will provide a sharper view of the marine hydrology system and of ocean dynamics.

Oceanographers have been collecting salinity data for over a century...allowing time-series construction for the better-sampled regions...

spatial and temporal images of SSS are poorly depicted by our overly smoothed maps constructed from decades of in situ observations. It is instructive to compare these blurry fields to the textured patterns revealed by satellite images of parameters such as sea surface temperature (SST), sea level, and sea-ice fields, and of wind stress acting on the ocean surface. Underway, in situ observations from research vessels reveal SSS spatial variability, which is perhaps even more textured than that of SST because SSS does not directly feed back to evaporation minus precipitation (E-P)—that is, when SSS increases, it doesn't induce more precipitation. However, underway data, while of potential value for process studies, do not provide a global view. A near-synoptic global view of SSS will be generated in the coming years as remote sensing of salinity from space is perfected, beginning with the 2008 launch of SMOS (European Soil Moisture and

Nevertheless, archived SSS data, albeit exhibiting gaps in space and time, may provide a reasonable record of the marine hydrological cycle since the mid-twentieth century. Others have used the archived data to study ocean salinity variability. For example, Curry et al. (2003) compared salinities on a long transect (50°S to 60°N) through the western Atlantic Ocean between the 1950s and 1990s. They found freshening at both poleward ends contrasted with increases of salinity pervading the upper water column, mostly the upper 500 m, at low latitudes. The positive anomaly is greatest in the 1990s. Boyer et al. (2006) examined large-scale trends in salinity from 1955 through 1998 for the world ocean and the Atlantic, Pacific, and Indian ocean basins from the surface to 3000-m depth, using oceanographic profile salinity measurements from the World Ocean Database 2001 (WOD1). Each basin exhibited large-scale, coher-

ent trends, with most of the North Pacific in the 15°S–60°N region freshening in the top 100 m, and with the same patterns and freshening noted by Curry et al. (2003) in the tropical and subtropical North Atlantic. Reverdin et al. (2007) mapped monthly SSS for the Atlantic Ocean from 30°S to 50°N, focusing on the better-sampled period from 1977 to 2002. They found that away from swift-current regions, SSS responds mostly to the local E-P and wind-induced Ekman transport, with a one- to two-month lag. They found long-lasting, larger-scale signals overlain on regional SSS variability. These are partly related to known climate signals, such as ENSO and the North Atlantic Oscillation (NAO).

ENSO explains ~ 20% of the interannual SSS variance in the western subtropical North Atlantic, while the NAO is better correlated with the interannual SSS (winter) fluctuations in the northeastern North Atlantic, near 40°–50°N (see Reverdin et al., 2007, Figures 13–15).

OBJECTIVES

The average salinity of the ocean's upper 20 m is a proxy for the marine hydrological cycle. SSS is akin to soil moisture, with an important difference: SSS is set not just by the freshwater sea-air fluxes but by overall ocean transfer

Arnold L. Gordon (agordon@ldeo.columbia.edu) is Associate Director, *Ocean and Climate Physics*, and Professor, *Earth and Environmental Sciences*, Lamont-Doherty Earth Observatory of Columbia University, Palisades, NY, USA.

Claudia F. Giulivi is Senior Staff Associate, *Ocean Climate and Physics*, Lamont-Doherty Earth Observatory of Columbia University, Palisades, NY, USA.

processes. In this study, we investigate aspects of the marine hydrological cycle as “seen” in fluctuations of subtropical SSS. These fluctuations are projected into the ocean subsurface by Ekman-induced downwelling, subduction, and convection. First, we use the archival hydrographic record averaged over the central region—the subtropical regimes of the North Atlantic and North Pacific (Figures 1 and 2). These data offer broad regional views of changing SSS patterns at the multiyear and decadal scales, though they lack clarity at the seasonal and interannual time scales. Next, we turn to the approximately monthly repeat observations of the water offshore of Bermuda for more temporal clarity (Figures 3 and 4), though they do not reveal spatial patterns. However, together these two views of SSS variability offer insight into the subtropical marine hydrological cycle of the North Atlantic Ocean with implied links to water-vapor telecommunication between the Atlantic and Pacific Oceans.

The effects of changing sea-air freshwater fluxes may be most evident in SSS time series where such fluxes are large compared to the freshwater fluxes brought about by ocean circulation and mixing. These sea-air freshwater fluxes occur in the central region of the large anticyclonic subtropical gyres, which are well removed from the ocean flux complications of the swift western boundary and equatorial currents and from the intense upwelling regime of the eastern boundary, and are remote from river plumes of the coastal environment. As archived SSS data are sparse in these regions, it is advantageous to combine data from a large area into a unified time series. This merging is best done where

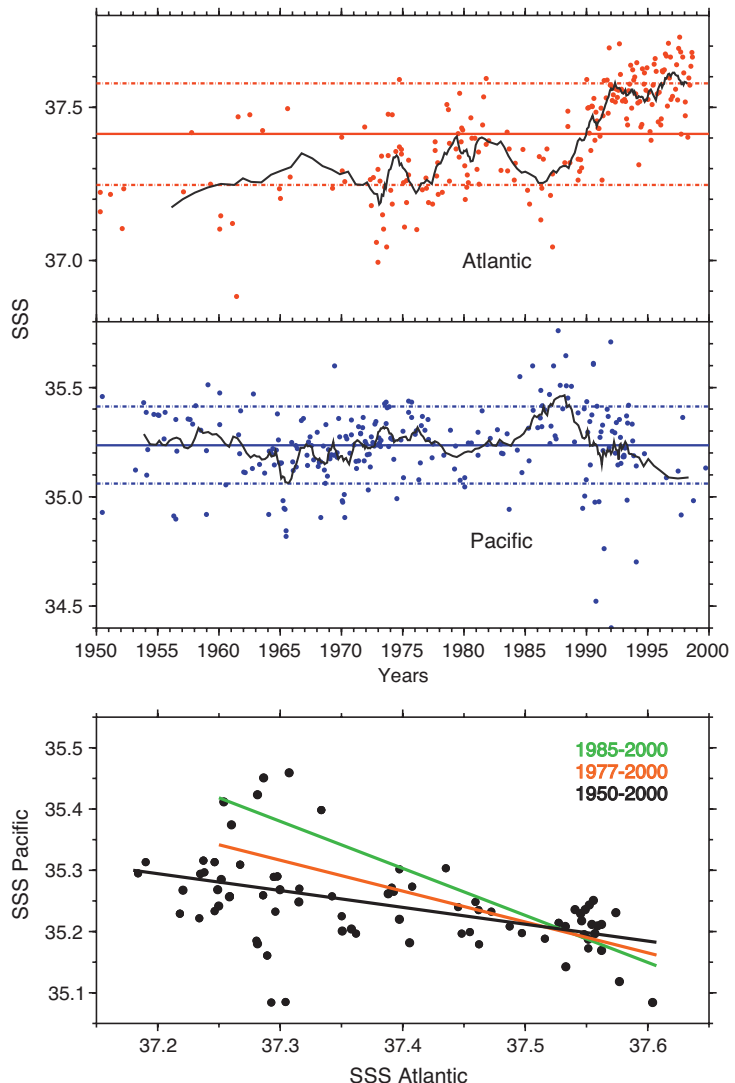


Figure 2. Upper panel: SSS time series for the central regions of the North Atlantic and North Pacific subtropical gyres shown in Figure 1. Circles represent the monthly averages of the data, and the solid black line is a 12-month running mean. Red and blue solid and dashed lines indicate the means and 1 standard deviation, respectively, of the monthly SSS data. Lower panel: North Pacific SSS versus North Atlantic SSS based on the 12-month running means. Solid lines represent the least-squares fit to the SSS averages for different periods.

the SSS lateral gradients are small, which is another attribute of the subtropical ocean (Figure 1). The subtropics are subject to net removal of freshwater by excess evaporation (E) over precipitation (P). Ocean processes compensate this $E-P$ by injecting lower-salinity

waters from the surrounding regions. Within the subtropical gyre, there is a net convergence of surface-layer water due to the Ekman transport. There is a general equatorial drift forced by the wind stress curl, called the meridional Sverdrup transport.

SEA-SURFACE SALINITY OF THE SUBTROPICAL NORTH ATLANTIC AND NORTH PACIFIC OCEANS

Oceanographers have been collecting salinity data for over a century (e.g., Antonov et al., 2006), allowing time-series construction for the better-sampled regions, at least for the last ~50 years. For this article, we

assembled SSS (upper 20 m) time series for the North Atlantic and North Pacific subtropical gyres (Figure 2) from data drawn mainly from the World Ocean Database 2005 (WOA05; Boyer et al., 2006). We also included surface-salinity observations from the WOCE Upper Ocean Thermal Data (UOT) and WOCE Sea Surface Salinity Data (both available from the WOCE Global Data Resource

Version 3.0, 2002).

Figure 2 shows that the Pacific Ocean attained a 50-year maximum SSS in 1988, and the Atlantic reached a minimum value in 1986. Since then, the Pacific and Atlantic subtropical SSSs have behaved in an inverse relationship—the Pacific SSS is freshening as the Atlantic becomes saltier (lower panel Figure 2). The slope of a linear fit of the North Atlantic to the North Pacific subtropical SSS for the period 1950–2000 is 0.25 (correlation coefficient of −0.47), increasing to a more significant 1.0 during the interval 1985–2000 (correlation coefficient of −0.68). Curry et al. (2003) also find that the positive salinity anomaly of the upper 500 m is greatest in the 1990s. The Pacific and Atlantic time series reveal temporal fluctuations, though these data are perhaps a bit too noisy from which to draw hard conclusions. The Bermuda time-series data provide more temporal information at their site within the western range of the North Atlantic subtropical SSS maximum.

SSS TIME SERIES NEAR BERMUDA

In 1954, Henry Stommel and colleagues started Hydrostation “S,” located 22 km southeast of Bermuda (Schroeder and Stommel, 1969; Joyce and Robbins, 1996), which is the longest continuous open-ocean time series. Since then, it has been visited biweekly, providing a hydrographic record nearly continuously through the present. The longevity and success of this deep-ocean time series led the Bermuda Institute of Ocean Sciences (BIOS, formerly BBSR) and the US Joint Global Ocean Flux Study (JGFO) to start the Bermuda Atlantic Time-series

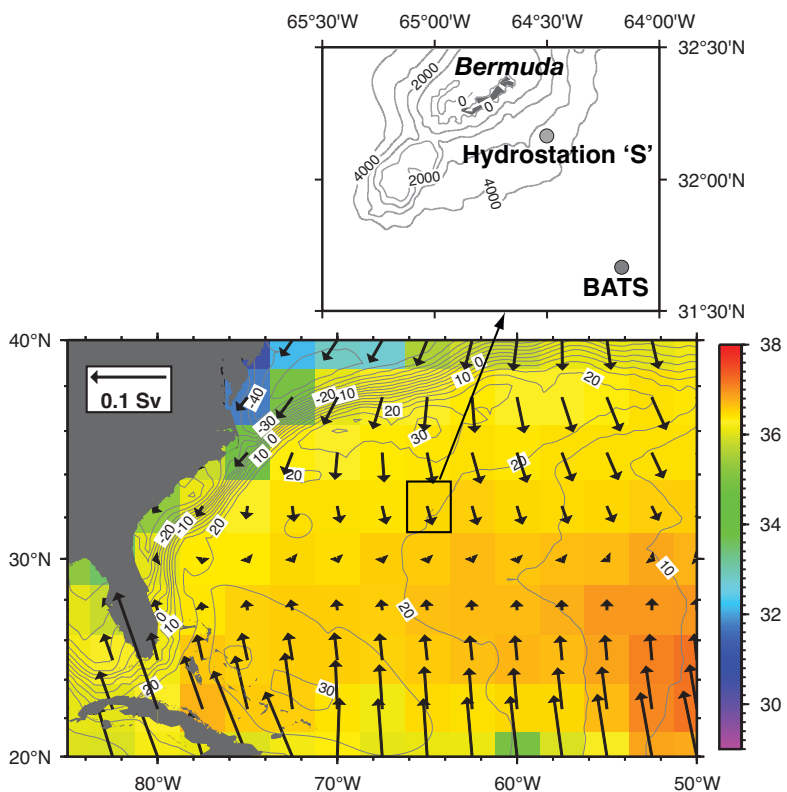


Figure 3. Ekman transport vectors in Sverdrups ($1 \text{ Sv} = 10^6 \text{ m}^3 \text{s}^{-1}$) and contours (every 5 cm) of mean dynamic ocean topography (MDOT) of the sea surface derived from jointly analyzed data from drifters, satellite altimetry, wind, and the GRACE (Gravity Recovery and Climate Experiment Mission) geoid model for the decade 1992–2002. The long-term mean SSS is in color. In the construction of the lower panel, Ekman transports were computed across $2.5^\circ \times 2.5^\circ$ latitude-longitude cells using long-term mean wind stresses based on ECMWF ERA-40 monthly data (Uppala et al., 2005). SSS (average salinity of the upper 20 m) was computed from the available hydrographic data from the World Ocean Database 2005 (WOA05; Boyer et al., 2006). Nikolai Maximenko (IPRC) and Peter Niiler (SIO) provided the 1992–2002 mean ocean dynamic topography data. The upper panel shows the location of the Bermuda Atlantic Time-series Study (BATS) and Hydrostation “S” sites in the Sargasso Sea (solid circles).

Study (BATS), another long-term time series that examines biogeochemical cycles in the Sargasso Sea near Bermuda. Hydrostation S and BATS data and reports are available online at <http://www.bats.bios.edu>. Numerous contributions that build upon the US JGOFS time-series stations and cover a full range of disciplines were the focus of two special issues of *Deep Sea Research Part II* (43[2–3] in 1996 and 48[8–9] in 2001).

The Pacific analog to BATS is the Hawaii Ocean Time-series (HOT) located at a deep-water site in the North Pacific subtropical gyre near Hawaii. It has been occupied since October 1988 at approximately monthly intervals, making repeated observations of the physics, biology, and chemistry of the water column (Karl and Lukas, 1996; http://www.soest.hawaii.edu/HOT_WOCE/).

Bermuda falls within a rather calm ocean current environment, situated well offshore of the Gulf Stream, with the vigorous eddy field of the Gulf Stream re-circulation gyre located immediately to its north (Figure 3; Steinberg et al., 2001; Fratantoni, 2001). We use BATS data collected from 1955 to 2003 to investigate SSS fluctuation in the western side of the North Atlantic subtropical regime (Figure 4). Because our objective is to use SSS as a proxy for the marine hydrological cycle, we do not delve into the subsurface strata. Several studies describe the temporal fluctuations of the water column observed at BATS, particularly the 18°C water that occurs at depths of a few hundreds meters, one of the major water masses formed in the northern Sargasso Sea in late winter (Worthington, 1959). Variability of this water mass, characterized by a layer of nearly constant density, has been used

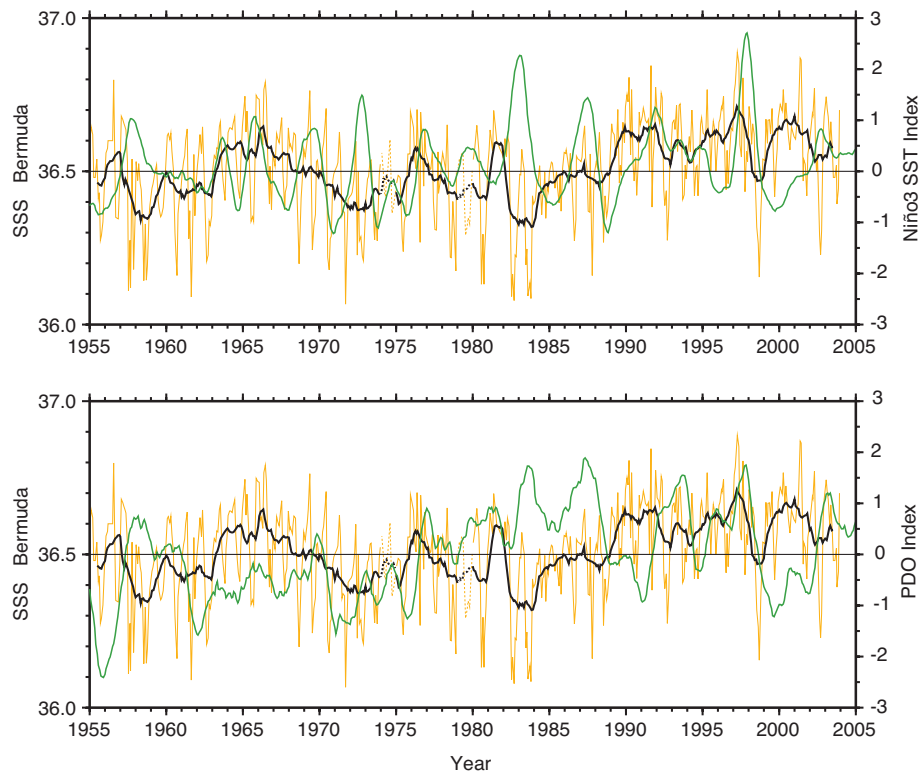


Figure 4. Monthly time series of SSS (orange line) from the combined Hydrostation S and BATS data for the period 1955–2003 (there are no data for 1979). The 12-month running mean of the combined SSS series is shown as a solid black line and a 12-month running mean of climate indices as a green line for Niño3 (upper panel) and Pacific Decadal Oscillation (PDO; lower panel).

as an indicator of climate variability over a much larger region of the western North Atlantic Ocean subtropical gyre (Talley and Raymer, 1982; Joyce and Robbins, 1996). Phillips and Joyce (2007) investigate the temperature, salinity, and density variability of the full water column at BATS from 1989 to 1999. They show that at BATS and Hydrostation S, the mean seasonal cycles of temperature, salinity, and density are indistinguishable and that the bulk of the seasonal signal is within the upper 20 m. These data support our use of the upper 20 m as representative of the storage of the seasonal freshwater. A weak seasonal salinity signal reaches 50–75 m in the fall season, which suggests interaction

of locally introduced freshwater to the subsurface layer, which, as Phillips and Joyce (2007) point out, appears to be subducted, local, saltier, winter surface water that is a component part of the local “hydrological regime.”

Changes in the monthly mean SSS and 12-month running mean using the BATS 1955–2003 data (Figure 4) reveal seasonal and interannual fluctuations. The average SSS over the 48-year time series is 36.51, with a standard deviation of 0.16. The monthly SSS attains its maximum value of 36.60 in the late winter and into early spring (February to April), which is a product of the winter evaporative predominance over precipitation. It achieves a minimum

of 36.39 in late summer and into early fall (August to October) due to summer rains. The average SSS seasonal range at BATS is 0.21 and corresponds to a freshwater inventory (upper 20 m) seasonal change of 0.12 m (meters of thickness of freshwater). However, the SSS seasonal range reveals significant interannual variability, from 0.1 to 0.4. Reverdin et al. (2007) average SSS maps for March and September in the Atlantic Ocean between 50°N and 30°S (see their Figure 3), showing that the seasonal SSS in the eastern North Atlantic subtropical gyre is opposite to that in the Bermuda area.

Over the 48-year record, looking at monthly resolution, the highest monthly SSS of 36.89 was attained in late winter 1997, with the minimum of 36.07 attained in the late summer of 1971. The range of 0.8 corresponds to a change in the freshwater inventory of 0.4 m within the upper 20 m. The 12-month running average has a more subdued 48-year range closer to 0.4 (minimum in 1984, maximum in 1997). Consistent with the North Atlantic subtropical SSS time series (Figure 2), the BATS data show that since 1988 the 12-month running mean SSS has been above the long-term average. This result provides confidence that the BATS time series portray the overall characteristics of the North Atlantic subtropical regime. A relatively salty period was also evident from 1963 to 1969, which is also suggested in the subtropical time series (Figure 2).

LOCAL E-P OR OCEAN FRESHWATER TRANSPORT?

Observed changes in the BATS SSS are due to fluctuations in the E-P and ocean transport of freshwater. The annual E-P

value in the Bermuda area is 0.2 m/year (NOAA NCEP-NCAR CDAS-1 monthly data; Kalnay et al., 1996). This value would increase the SSS 0.36 per year were it not for the compensating effect of freshwater convergence by ocean advection and mixing. Because Bermuda is slightly north of the subtropical convergence, Ekman transport is weak and directed from north to south (Figure 3). The mean geostrophic flow is also weak and is directed from the northeast to the southwest (Figure 3). The SSS gradient to the north of Bermuda is $4 \times 10^{-7} \text{ m}^{-1}$. The average speed of surface flow from the north as required to balance the yearly E-P-induced increase in SSS is approximately 2 cm/sec. Surface-drifter (drogued at 15 m) maps indicate currents in the Bermuda region of ~ 1.4 cm/sec with an uncertainty ellipse of ± 1.7 cm/sec (see <http://www.aoml.noaa.gov/phod/dac/gdp.html>). This value is close to the required 2 cm/sec. Surface-layer flow associated with Ekman transport in the BATS region (Figure 3) is small (0.3 cm/sec). Sverdrup transport ($M_y = -\text{wind stress curl}/\beta$, where β is the meridional gradient of the Coriolis parameter) across the North Atlantic near the Bermuda latitude is ~ 30 Sv (Mayer and Weisberg, 1993; Tomczak and Godfrey, 2003, see their figure 4.7 on the text Web site: <http://gyre.umeoce.maine.edu/physicalocean/Tomczak/regoc/pdfversion.html>), which is matched approximately by a transport of 30 to 34 Sv through the Florida Strait (Baringer and Larsen, 2001). This uniformly distributed transport across the width of the North Atlantic for the upper 1000 m yields a southward speed of 0.4 cm/sec. The sum of the Ekman

and Sverdrup transport speeds at the Bermuda site agrees with the satellite drifter data, but it is barely one half of the required advective freshwater flux. The remainder may be attributed to fluxes associated with the energetic mesoscale eddy field of the Gulf Stream recirculation gyre immediately to the north of Bermuda (Frantoni, 2001).

As mentioned above, without the compensating ocean transport of freshwater, the Bermuda SSS would increase annually by 0.36. The interannual variability (12-month running mean) of SSS is 0.4, approximately the effect of the climatic E-P if the ocean transport were to disappear. Surface drifter data do not reveal such large long-term fluctuations of the surface current. Therefore, while there is uncertainty, we propose that the bulk of the observed SSS variability in the Bermuda region is due to changes in regional E-P. If part of the Bermuda SSS change were due to ocean transport variability, it would be, to a large measure, a reflection of the regional-scale E-P control of SSS. The fact that the precipitation along the US Gulf Coast follows a similar relationship to ENSO (discussed below; Figure 5), as does the Bermuda SSS time series, supports this speculation.

NORTH ATLANTIC SUBTROPICAL SSS AND ENSO

The BATS data offer the opportunity to investigate interannual variability of the regional hydrological cycle. As SSS is an integrated measure of E-P variations, its time-derivative is better phased than SSS itself with climate indices that are associated with these E-P variations. The SSS rate of change based on the 12-month running mean of monthly BATS data is compared to SST anomalies for the

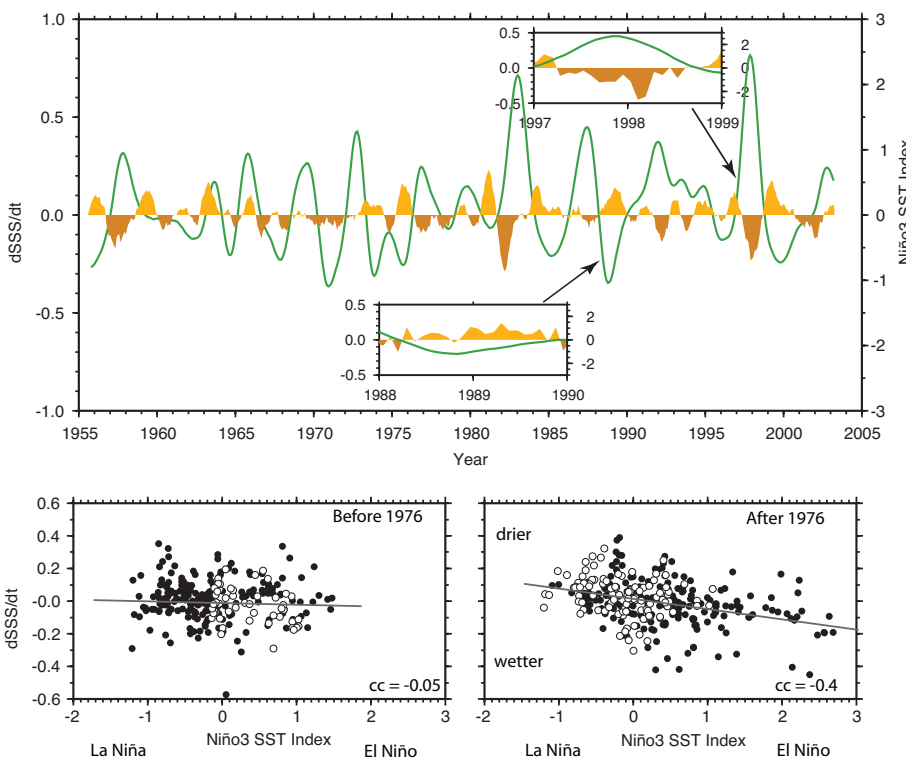


Figure 5. Upper panel: Monthly rate of change of SSS with the high-frequency fluctuations smoothed by the application of two running means: first, an eight-month running mean and then a twelve-month running mean. The same procedure was done on Niño3, green line. The lighter-orange color denotes a positive rate of change of SSS values (increasing SSS with time), while brown denotes a negative rate of change (decreasing SSS with time). The two boxes in the upper panel display a more detailed view of a period of decreasing SSS, which corresponds to the strong El Niño event of 1997/1998, and increasing SSS corresponding to the strong La Niña event of 1989. For these data, a single 12-month running mean filter was applied. Lower panels: Monthly SSS change vs. Niño3 for the period 1955–1976 (left) and 1977–2003 (right). These data points are from a single 12-month running mean filter output. Open circles show positive (negative) PDO values during a negative (positive) PDO phase before (after) 1976. Correlation coefficients are indicated in the panels.

Niño3 region of 5°N–5°S, 90°W–150°W (Kaplan et al., 1998). A positive Niño3 is indicative of an El Niño event. We find that changes in BATS SSS reveal a fairly robust relationship to ENSO (Figure 6): during El Niño there is a reduction of SSS, while La Niña denotes times of increasing SSS. The 12-month running mean for the Niño3 index bears an inverse relationship to the 12-month running mean of SSS rate of change. This correlation is shown in more detail in the

two boxes in the upper panel of Figure 6, which clearly display a period of decreasing SSS that corresponds to a strong El Niño event (1998) and increasing SSS that corresponds to a strong La Niña event (1989). Unexpectedly, this relationship is robust only after 1976 (lower panels of Figure 6). That year marks the well-known climate-regime shift when the Pacific Decadal Oscillation (PDO) entered into a prolonged period of positive phase (Trenberth and

Hurrell, 1994; Latif and Barnett, 1994; Mantua et al., 1997).

The HOT time series data reveal, as expected, that ENSO and PDO affect rainfall patterns over the subtropical North Pacific (Lukas, 2001), which are projected into the subsurface layers by subduction (Lukas and Santiago-Mandujano, this issue). We now show that these climate features also affect the subtropical North Atlantic.

Regional E-P values may be further explored with the NOAA NCEP-NCAR CDAS-1 monthly data (Kalnay et al. 1996). The E-P values are determined using surface heat latent flux and surface precipitation rate products from the NCEP data. Figure 5 shows correlation maps between subtropical North Atlantic E-P and the Niño3 Index. The 90% significance level is 0.3. The December-January-February period is shown because in that season, the rainfall over the US Gulf Coast reveals the strongest correlation to ENSO (Ropelewski and Halpert, 1986, and see: <http://www.cpc.ncep.noaa.gov/products/precip/CWlink/ENSO/total.shtml>). Since 1976, the US Gulf Coast and the entire ocean subtropical region display a negative correlation to Niño3: during El Niño, the E-P anomaly is negative, meaning less evaporation or more precipitation. This inference is consistent with reduced SSS during El Niño as revealed by the BATS data. Prior to 1976, the regional (including the Gulf Coast) E-P has a mixed correlation with Niño3, with some areas exhibiting a positive correlation, and other areas a negative correlation. These data suggest that PDO might affect the projection of El Niño into the subtropical North Atlantic and Gulf Coast states. Caution in draw-

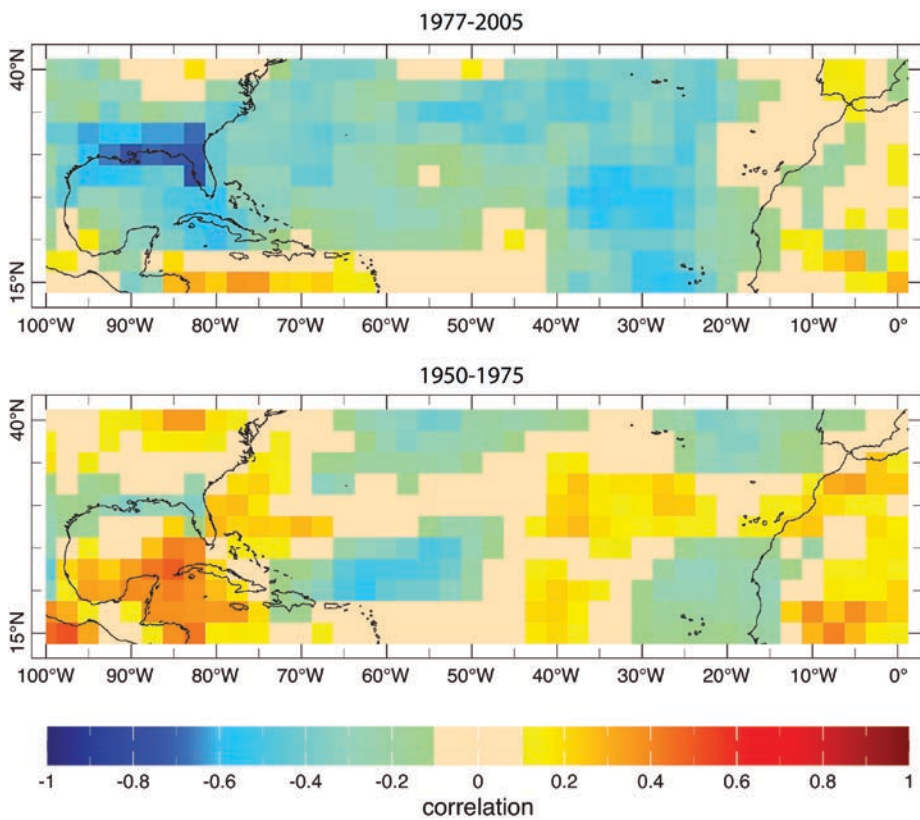


Figure 6. Winter (December–January–February) correlation maps between subtropical North Atlantic evaporation minus precipitation ($E-P$) and Niño3 Index for the period 1977–2005 (upper panel) and 1950–1975 (lower panel). This winter period is shown because in that season, the rainfall over the US Gulf Coast reveals the strongest correlation to ENSO. Atmospheric data are from the National Centers for Environmental Prediction.

ing this conclusion is recommended because the NCEP data prior to 1979 (when satellite data were drawn into the analysis) are not as accurate as they are after 1979. However, one may expect the $E-P$ values along the Gulf Coast, where there are adequate weather stations, to be reasonably accurate. Correlation maps (not shown) of Niño3 with winter (December–February) precipitation data from different sources, including observational and re-analysis data (GPCP, Version 2 of the Combined Precipitation Data; NOAA NCEP CPC PRECL; NCEP–NCAR CDAS-1; ECMWF ERA-40; NOAA CPCP Merged Analysis version2), display significant positive

correlation values in the Gulf of Mexico, with higher correlation values after 1977. Some studies of Pacific Ocean-derived moisture fluxes over the Americas (e.g., Mestas-Nunez et al., 2007) find that during the winter, the moisture delivered to the United States is derived from the Pacific with some contribution from the Gulf of Mexico; winter interannual variability is affected by ENSO, and possibly by the North Atlantic Oscillation (NAO). Gershunov and Barnett (1998) show that the North Pacific Oscillation (NPO, or PDO) exerts a modulating effect on ENSO teleconnections. Typical El Niño patterns are strong and consistent only during the high phase of the NPO

(+PDO, as we find in this paper based on SSS fluctuations). For the moisture flux link between PDO and ENSO, these authors suggest that a deeper Aleutian low (characteristic of a +PDO) shifts the storm track southward while El Niño provides an enhanced eastern tropical Pacific moisture source for the storms to tap. Gershunov and Barnett (1998) say in their concluding paragraph: “The central implication of this paper is that stratification of ENSO-based statistical forecasts by the NPO (PDO) phase should greatly enhance the accuracy of such forecasts, particularly in the western and central United States.”

CONCLUSION

Sea-surface salinity has great potential to help define the marine hydrological cycle. The archived hydrographic data within the hub of the North Atlantic subtropical gyre and higher temporal resolving time series of BATS show, perhaps not surprisingly, that the SSS of the subtropical North Atlantic fluctuates at interannual and decadal time scales. The North Atlantic subtropical SSS is getting saltier since the mid to late 1980s while the North Pacific subtropical SSS is getting fresher. We suggest that these changes are due to $E-P$, though changes in ocean circulation may also be a factor. Both ENSO and PDO affect the subtropical North Atlantic SSS. ENSO and PDO influences appear to be linked: we find that the projection of El Niño into the subtropical North Atlantic is much more robust when PDO is in a positive phase, as has been the situation since 1976. The cause for this apparent (atmospheric) telecommunication of the Pacific climate into the subtropical North Atlantic requires further consideration.

Our intent in this study is to show the power of salinity, notably of SSS, in the study of the poorly known aspect of Earth's climate system, the marine hydrological cycle.

Might the observed decadal SSS trends within the subtropical North Atlantic and North Pacific be related to ENSO and PDO changes in water-vapor transport across Central America? Does this transport affect the deep Atlantic meridional overturning circulation? What is the response of shallow subtropical meridional overturning circulation and associated heat flux to the SSS trends of the subtropical gyre?

ACKNOWLEDGEMENTS

This work was supported by NASA grant NNX06AD57G. Thoughtful comments from the reviewers are gratefully acknowledged. Special thanks to all personnel involved at BATS and HOT and the funding provided by different agencies to keep these projects providing continuously valuable data. Lamont-Doherty Earth Observatory contribution number 7115. ☐

REFERENCES

- Antonov, J.I., R.A. Locarnini, T.P. Boyer, A.V. Mishonov, and H.E. Garcia. 2006. *World Ocean Atlas 2005, Volume 2: Salinity*. S. Levitus, ed., NOAA Atlas NESDIS 62, US Government Printing Office, Washington, DC, 182 pp.
- Baringer, M., and J. Larson. 2001. Sixteen years of Florida Current Transport at 27°N. *Geophysical Research Letters*, 28(16):3,179–3,182.
- Baumgartner, A., and E. Reichel. 1975. *The World Water Balance: Mean Annual Global, Continental and Maritime Precipitation*. Elsevier, Amsterdam, The Netherlands, 179 pp.
- Boyer T.P., J.I. Antonov, H.E. Garcia, D.R. Johnson, R.A. Locarnini, A.V. Mishonov, M.T. Pitcher, O.K. Baranova, and I.V. Smolyar. 2006. *World Ocean Database 2005*. S. Levitus, ed., NOAA Atlas NESDIS 60, US Government Printing Office, Washington, DC, 190 pp., DVDs.
- Curry, R., B. Dickson, and I. Yashayaev. 2003. A change in the freshwater balance of the Atlantic Ocean over the past four decades. *Nature* 426:826–829.
- Fratantoni, D.M. 2001. North Atlantic surface circulation during the 1990s observed with satellite-tracked drifters. *Journal of Geophysical Research* 106:22,067–22,094.
- Gershunov, A., and T. Barnett. 1998. Interdecadal modulation of ENSO teleconnections. *Bulletin of the American Meteorological Society* 79(12):2,715–2,725.
- Gordon, A.L. 2001. Intercean exchange. Pp. 303–314 in *Ocean Circulation and Climate*, G. Siedler, J. Church, and J. Gould, eds, Academic Press, London.
- Joyce, T., and P. Robbins. 1996. The long-term hydrographic record at Bermuda. *Journal of Climate* 9:3,121–3,131.
- Kalnay, E., M. Kanamitsu, R. Kistler, W. Collins, D. Deaven, L. Gandin, M. Iredell, S. Saha, G. White, J. Woollen, and others. 1996. The NMC/NCAR 40-year reanalysis project. *Bulletin of American Meteorological Society* 77:437–471.
- Kaplan, A., M. Cane, Y. Kushnir, A. Clement, M. Blumenthal, and B. Rajagopalan. 1998. Analyses of global sea surface temperature 1856–1991. *Journal of Geophysical Research* 103:18,567–18,589.
- Karl, D.M., and R. Lukas. 1996. The Hawaii Ocean Time-series (HOT) Program: Background, rationale and field implementation. *Deep-Sea Research Part II* 43:129–156.
- Lagerloef, G., C. Swift, and D. Le Vine. 1995. Sea surface salinity: The next remote sensing challenge. *Oceanography* 8:44–50.
- Latif, M., and T.P. Barnett. 1994. Causes of decadal climate variability over the North Pacific and North America. *Science* 266(5185):634–637.
- Lukas, R. 2001. Freshening of the upper thermocline in the North Pacific subtropical gyre associated with decadal changes of rainfall. *Geophysical Research Letters* 28:3,485–3,488.
- Mantua, N.J., S.R. Hare, Y. Zhang, J.M. Wallace, and R.C. Francis. 1997. A Pacific interdecadal climate oscillation with impacts on salmon production. *Bulletin of the American Meteorological Society* 78:1,069–1,079.
- Mayer, D.A., and R.H. Weisberg. 1993. A description of COADS surface meteorological fields and the implied Sverdrup transports for the Atlantic Ocean from 30°S to 60°N. *Journal of Physical Oceanography* 23:2,201–2,221.
- Mestas-Nuñez, A., D. Enfield, and C. Zhang. 2007. Water vapor fluxes over the Intra-Americas Sea: Seasonal and interannual variability and associations with rainfall. *Journal of Climate* 20(9):1,910–1,922.
- Phillips, H., and T. Joyce. 2007. Bermuda's Tale of Two Time Series: Hydrostation S and BATS. *Journal of Physical Oceanography* 37:554–571.
- Reverdin, G., E. Kestenare, C. Frankignoul, and T. Delcroix. 2007. Surface salinity in the Atlantic Ocean (30°S–50°N). *Progress in Oceanography* 73:311–340.
- Ropelewski, C.F., and M.S. Halpert. 1986. North American precipitation and temperature associated with the El Niño/Southern Oscillation (ENSO). *Monthly Weather Review* 114:2,352–2,362.
- Schmitt, R., P. Bogden, and C. Dorman. 1989. Evaporation minus precipitation and density fluxes for the North Atlantic. *Journal of Physical Oceanography* 10:1,210–1,221.
- Schmitt, R.W. 1995. The ocean component of the global water cycle. *Reviews of Geophysics* 33(Suppl., Pt. 2):1,395–1,409.
- Schroeder, E., and H. Stommel. 1969. How representative is the series of *Panulirus* stations of monthly mean conditions off Bermuda? *Progress in Oceanography* 5:31–40.
- Steinberg, D., C. Carlson, N. Bates, R. Johnson, A. Michaels, and A. Knap. 2001. Overview of the US JGOFS Bermuda Atlantic Time-Series Study (BATS): A decade-scale look at ocean biology and biogeochemistry. *Deep-Sea Research Part II* 48(8):1,405–1,447.
- Talley, L., and M.E. Raymer. 1982. Eighteen degree water variability. *Journal of Marine Research* 40(Suppl.):757–775.
- Tomczak, M., and J.S. Godfrey. 2003. *Regional Oceanography: An Introduction*, 2nd ed. Daya Publishing House, Delhi. Available online at: <http://gyre.umeoce.maine.edu/physicalocean/Tomczak/regoc/pdfversion.html> (accessed December 19, 2007).
- Trenberth, K.E., and J.W. Hurrell. 1994. Decadal atmosphere-ocean variations in the Pacific. *Climate Dynamics* 9:303–319.
- Uppala, S.M., P.W. Kallberg, A.J. Simmons, U. Andrae, V. Da Costa Bechtold, M. Fiorino, J.K. Gibson, J. Haseler, A. Hernandez, G.A. Kelly, and others. 2005. The ERA-40 re-analysis. *Quarterly Journal of the Royal Meteorological Society* 131:2,961–3,012.
- U.S. CLIVAR. 2007. Report of the US CLIVAR salinity science working group. US CLIVAR Report No. 2007-1, US CLIVAR Office, Washington DC, 46 pp.
- Worthington, L.V. 1959. 18 degree water in the Sargasso Sea. *Deep-Sea Research* 5:297–305.
- Worthington, L.V. 1981. The water masses of the world ocean: Some results of a fine-scale census. Pp. 43–69 in *Evolution of Physical Oceanography*. B. Warren and C. Wunsch, eds, MIT Press, Cambridge, MA.